



Get Clarity On Generics

Cost-Effective CT & MRI Contrast Agents

 FRESENIUS
KABI

WATCH VIDEO

AJNR

Fluid-Attenuated Inversion-Recovery MR Imaging in Acute and Subacute Cerebral Intraventricular Hemorrhage

Rohit Bakshi, Sadaat Kamran, Peter R. Kinkel, Vernice E. Bates, Laszlo L. Mechtler, Vallabh Janardhan, Shaleen L. Belani and William R. Kinkel

This information is current as of August 20, 2025.

AJNR Am J Neuroradiol 1999, 20 (4) 629-636
<http://www.ajnr.org/content/20/4/629>

Fluid-Attenuated Inversion-Recovery MR Imaging in Acute and Subacute Cerebral Intraventricular Hemorrhage

Rohit Bakshi, Sadaat Kamran, Peter R. Kinkel, Vernice E. Bates, Laszlo L. Mechtler, Vallabh Janardhan, Shaleen L. Belani, and William R. Kinkel

BACKGROUND AND PURPOSE: Fluid-attenuated inversion-recovery (FLAIR) MR imaging may show subarachnoid hemorrhage (SAH) with high sensitivity. We hypothesized that the FLAIR technique is effective and reliable in the diagnosis of cerebral intraventricular hemorrhage (IVH).

METHODS: Two observers evaluated the 1.5-T MR fast spin-echo FLAIR images, T1- and T2-weighted MR images, and CT scans of 13 patients with IVH and the FLAIR images of 40 control subjects.

RESULTS: IVH appeared bright on the FLAIR images obtained during the first 48 hours and was of variable appearance at later stages. FLAIR MR imaging detected 12 of 13 cases of IVH; no control subjects were falsely thought to have IVH (92% sensitivity, 100% specificity). However, IVH could not be fully excluded in the third ventricle (20%, $n = 8$) or in the fourth ventricle (28%, $n = 11$) on some control images because of CSF pulsation artifacts. Two cases had CT-negative IVH seen on FLAIR images. One case had FLAIR-negative IVH seen by CT. Although the sensitivities of conventional MR imaging (92%) and CT (85%) were also high, FLAIR imaging showed IVH more conspicuously than did standard MR imaging and CT in 62% of the cases ($n = 8$). FLAIR was as good as or better than CT in showing IVH in 10 cases (77%). FLAIR images showed all coexisting SAH.

CONCLUSION: FLAIR MR imaging identifies acute and subacute IVH in the lateral ventricles with high sensitivity and specificity. In cases of subacute IVH, conventional MR imaging complements FLAIR in detecting IVH. The usefulness of the FLAIR technique for detecting third and fourth ventricular IVH may be compromised by artifacts. Blood hemoglobin degradation most likely causes the variable FLAIR appearance of IVH after the first 48 hours.

CT has long been the neuroimaging study of choice to exclude acute intracerebral hemorrhage (ICH) (1), especially subarachnoid hemorrhage (SAH) (2). Most recently, the development of the MR fluid-attenuated inversion-recovery (FLAIR) technique and the ability to perform FLAIR with a fast spin echo (fast FLAIR) has markedly improved the detection of a variety of brain disorders as compared with conventional MR imaging (3). The superiority of FLAIR relates to its sensitive detection of lesions causing T2 prolongation with nulling of normal CSF background, leading to high lesion/tis-

sue contrast (4). The usefulness of FLAIR as compared with T1- and T2-weighted MR imaging has been shown in association with a host of brain diseases, including stroke (4, 5), multiple sclerosis (6, 7), infections (8, 9), hypertensive encephalopathy/reversible posterior leukoencephalopathy syndrome (10), and myotonic dystrophy (11). In addition, one group has shown that FLAIR imaging may be reliable in the diagnosis of acute SAH and may be superior to CT in this regard (12–14). The role of FLAIR in the diagnosis of other types of ICH has not been established. In the present study, we tested the hypothesis that the fast FLAIR technique would be effective and reliable in the diagnosis of acute and subacute cerebral intraventricular hemorrhage (IVH), with high sensitivity and specificity.

Methods

Subjects

Our adult tertiary hospital neuroimaging computer database was reviewed to identify all cases of IVH that were observed

Received September 8, 1998; accepted after revision December 22.

From the Dent Neurologic Institute, Lucy Dent Imaging Center, Kaleida Health System, Millard Fillmore Hospital, State University of NY, Buffalo, NY.

Address reprint requests to Rohit Bakshi, MD, Lucy Dent Imaging Center, 3 Gates Circle, Buffalo, NY 14209.

© American Society of Neuroradiology

during a 1-year period (May 1997 through April 1998). We searched the database to identify all patients with IVH who had undergone both cranial MR imaging and CT. Clinical information in the patients' medical charts was reviewed to determine age, sex, associated illnesses, and presenting symptoms. IVH was diagnosed by a sudden change in neurologic status and the presence of either angiographically documented arteriovenous malformation (AVM)/aneurysm or MR- or CT-documented coexisting acute ICH. Time of IVH onset (ictus) was defined as the time of the sudden appearance of new neurologic symptoms. We excluded patients whose CT and MR studies were not obtained within 24 hours of each other, whose ictus was not definitively known, who had neoplastic, post-operative, or infectious brain diseases, and whose images were of poor quality. The Human Research Committee at our institution approved this study.

Imaging

MR imaging was performed on a Phillips ACS-NT 1.5-T fast scanner (Phillips Medical Systems, Eindhoven, The Netherlands). Fast FLAIR parameters were as follows: 6700/150/2 (TR/TE/excitations), inversion time (TI), 2200; fast spin echo, 20; field of view, 24 cm; matrix, 189 × 256; 5-mm-thick axial sections; and a scan time of approximately 2 minutes. Conventional MR axial noncontrast T1-weighted images (450/20/2) and fast spin-echo T2-weighted images (2000/120/2) were also obtained. CT was performed using noncontrast axial sections.

Two experienced raters who were unaware of the clinical details analyzed the MR and CT appearance and conspicuousness of IVH and coexisting SAH. The presence of IVH was noted, and the predominant signal quality of the IVH on the FLAIR and the T1- and T2-weighted images in relation to cortical gray matter was classified as hypointense, hyperintense, isointense, or mixed (containing hypointense and hyperintense portions). A visual comparison was then made for each patient to determine which study (FLAIR, T1-weighted, T2-weighted, or CT) best showed the IVH, coexisting SAH, or both. Contrast-enhanced MR imaging or CSF analysis was not performed in any of the patients. Two raters who were unaware of the clinical details also analyzed the FLAIR images of 40 age-matched control subjects for findings consistent with IVH. The lateral ventricles, third ventricle, and fourth ventricle in the control subjects were rated as follows: grade 0, normal hypointense signal; grade 1, equivocal (probable artifact but unable to fully exclude small focal IVH); and grade 2, definite IVH. The control subjects underwent FLAIR MR imaging for evaluation of headache, seizure disorder, or dizziness; the results in the original reports (previously interpreted for the hospital officially by the coauthors) were normal in all cases. Disagreements between raters were resolved by consensus.

Results

General Features

General features are summarized in the Table. Thirteen patients with IVH, ages 24 to 82 years (mean, 60 years), were identified. Six (48%) were men. Neuroimaging was performed at various times ranging from the same day of ictus (day 0) to day 11 after ictus (mean, 3.6 days). Five patients were studied within 48 hours of ictus, defined as the acute stage (day 0 or day 1). IVH was caused by hypertension (n = 5), aneurysms (n = 2), AVMs (n = 2), or idiopathic causes (n = 4). Amyloid angiopathy, unrecognized hypertension, or alcoholism may have explained idiopathic cases. All

MR and CT findings in 13 patients with cerebral intraventricular hemorrhage: role of FLAIR

Case No.	Age	IVH Cause	Coexisting Hemorrhage	Ictus (days)	IVH Location	MR Appearance			IVH Conspicuousness		Diagnosis by Raters		
						T1	T2	FL	FL vs CT	MR vs CT	FLAIR	T1, T2	CT
1	40	HTN	IPH putamen	0	LLV	↔	↑	↑	FL>CT	FL	IVH	IVH	IVH
2	43	Idiopathic	IPH,SAH	0	BLV	↔	↔↑	↔↑	FL>CT	FL	IVH	IVH	IVH
3	79	HTN	IPH cerebellum	1	BLV	↔	↔	↑	FL>CT	FL	IVH	IVH	IVH
4	58	Idiopathic	IPH temporal,SAH	1	LLV	↔	→	↑	FL>CT	FL	IVH	IVH	IVH
5	49	MCA aneurysm	IPH,SAH	1	BLV	↔	↔	↑	FL>CT	FL	IVH	IVH	N/D
6	81	Idiopathic	IPH,SAH	2	BLV	↔	↔	↑	FL>CT	FL	IVH	IVH	IVH
7	24	AVM	None	2	LLV	↑	→	→	CT>FL	T1=CT	IVH	IVH	IVH
8	67	HTN	IPH	3	RLV	↑	→	→	CT>FL	T1	IVH	IVH	IVH
9	82	HTN	IPH	5	BLV	↔	↔	↔	CT>FL	CT	N/D	N/D	IVH
10	51	Idiopathic	IPH frontal	7	BLV	↔↑	↔	↔	FL>CT	FL	IVH	IVH	IVH
11	29	AVM	None	8	BLV,3	↑	↓↑	↓↑	FL=CT	T1	IVH	IVH	IVH
12	70	BA aneurysm	SAH	9	BLV	↔	↔	↑	FL>CT	FL	IVH	IVH	IVH
13	63	HTN	IPH thalamus	11	RLV,3	↔	↔	↔↑	FL>CT	T2	IVH	IVH	N/D

Note.—FL vs CT indicates FLAIR to CT comparison of IVH detection; MR vs CT, MR (FLAIR,T1,T2) to CT comparison of IVH detection; ↓, hypointense; ↔↑, mildly hyperintense; ↑, hyperintense; ↓↑, hypointense and hyperintense (mixed); 3, third ventricle; AVM, arteriovenous malformation; BA, basilar artery; BLV, bilateral lateral ventricles; CT, noncontrast CT scan; FL, FLAIR; HTN, hypertension; ictus, interval between symptom onset and MR; IPH, intraparenchymal hemorrhage; IVH, intraventricular hemorrhage; LLV, left lateral ventricle; MCA, middle cerebral artery; N/D, IVH not diagnosed; RLV, right lateral ventricle; SAH, subarachnoid hemorrhage; T1, T1-weighted images; T2, T2-weighted images.

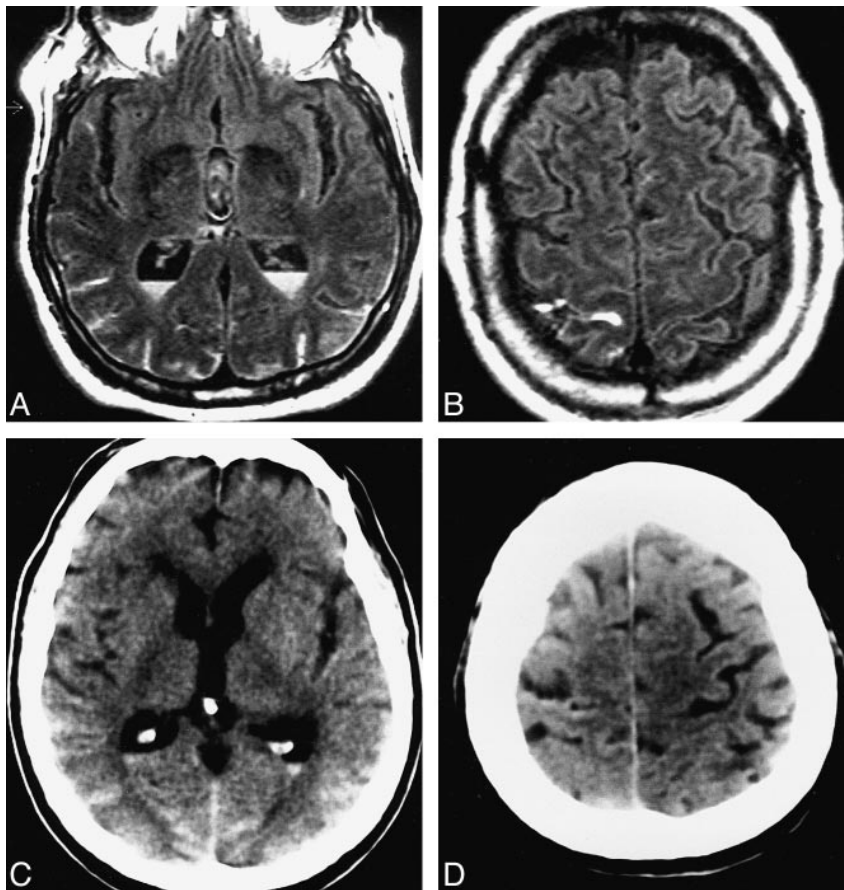


FIG 1. Case 12: 70-year-old man with subacute aneurysmal IVH and SAH who had MR imaging 9 days after ictus and CT 8 days after ictus. The FLAIR images show each occurrence of hemorrhage more conspicuously than do the CT scans. Although both FLAIR MR imaging and CT depicted IVH, the FLAIR images more crisply show the fluid-fluid levels characteristic of IVH.

A and B, FLAIR images (6700/150/2, T1 = 2200) show layered IVH in the trigones of the lateral ventricles, which are hyperintense (A), resulting in blood-CSF fluid-fluid levels. Mixed intensities in the third ventricle are most likely caused by CSF pulsation artifact (and were also seen on the control images). Hyperintense posterior or bilateral parietal and occipital (A) and right rolandic (B) cortical sulci represent SAH.

C and D, Noncontrast CT scans show both the IVH and SAH less conspicuously than do the FLAIR images, including layered IVH (C), bilateral parietooccipital SAH (C), and right rolandic sulcus SAH (D).

aneurysms and AVMs were confirmed by conventional angiography. Eleven patients with IVH had coexisting ICH at MR imaging/CT, including intraparenchymal hemorrhage ($n = 10$), SAH ($n = 5$), or both ($n = 4$). Two cases of IVH were observed without coexisting ICH on MR/CT studies, and both were caused by AVMs. IVH always involved the lateral ventricles ($n = 13$), usually bilaterally ($n = 8$). Two patients had third ventricular IVH; each had coexisting lateral ventricular IVH. None of the patients had fourth ventricular IVH. Hydrocephalus was uncommon (15%, $n = 2$). Serial MR imaging of two patients showed resolution of IVH at 20 and 50 days after ictus.

Imaging Features

MR imaging findings are shown in the Table and in Figures 1–4. FLAIR detected 12 of the 13 cases of IVH, and none of the FLAIR images of the control subjects falsely depicted IVH (92% sensitivity, 100% specificity). Two patients had negative CT results although their FLAIR images showed IVH. Although sensitivities of conventional MR imaging (92%) and CT (85%) were also high, FLAIR images showed IVH more conspicuously than did T1- and T2-weighted MR images and CT scans for 62% of the patients ($n = 8$) (Figs 1 and 3). FLAIR imaging was as good as ($n = 1$) or better than ($n = 9$) CT in showing IVH for 10

patients (77%). T1-weighted ($n = 3$) or T2-weighted ($n = 1$) MR images showed IVH better than the FLAIR images did in some instances. CT was better than FLAIR for three patients (23%) (Figs 2 and 4), one of whom had IVH that was diagnosed only by CT (Fig 4).

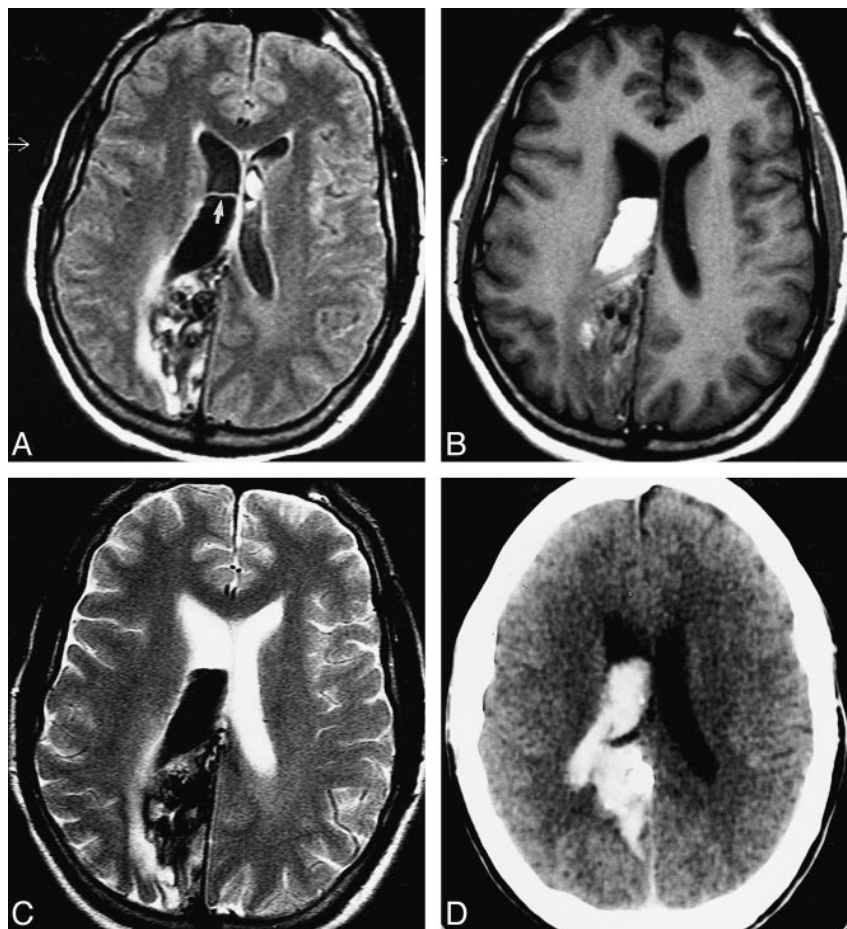
IVH was most commonly seen as layered fluid-fluid levels in the dependent portions of the ventricles. IVH usually appeared hyperintense on FLAIR images (69%, $n = 9$), and thus was easy to see against a dark CSF background (Figs 1 and 3). The FLAIR appearance was variable depending on time since ictus. All IVH appeared hyperintense on the FLAIR images obtained during the first 48 hours (day 0 or day 1) ($n = 4$) (Figs 1 and 3). After 48 hours, isointense ($n = 1$), mixed ($n = 1$), and hypointense ($n = 2$) (Fig 2) IVH appearances were also seen on the FLAIR images. When isointense or hypointense on the FLAIR images, IVH was more difficult to visualize but might have been easily seen on T1- or T2-weighted images (Fig 2). Isointense or hypointense IVH on the FLAIR images was associated with an isointense or hyperintense appearance on the T1-weighted images and an isointense or hypointense appearance on the T2-weighted images, suggesting the conversion to deoxyhemoglobin and/or intracellular methemoglobin. Coexisting SAH ($n = 5$) was well seen at all stages as a hyperintense signal on the FLAIR images (Figs 1 and 3). Third ventricular IVH ($n = 2$)

FIG 2. Case 7: 24-year-old man with acute IVH and intraparenchymal hemorrhage who had MR imaging and CT 12 hours apart, each approximately 72 hours after ictus. Although the IVH is more easily seen on the CT scans than on the FLAIR images, the T1-weighted images show the IVH as well as the CT scans do.

A, FLAIR image (6700/150/2, $T_1 = 2200$) shows a marked hypointensity, consistent with clot, in the posterior aspect of the right lateral ventricle. The linear meniscus (arrow) demarcates the posterior clot from the normal anterior CSF signal. The marked hypointensity of the IVH is most likely caused by the T2 shortening effects of intracellular methemoglobin present abundantly in the clot at this IVH stage. The hypointensity of this state of blood breakdown resembles normal dark CSF. In addition, heterogeneous signal is present in the mesial part of the right parietooccipital lobe with surrounding hyperintensity, consistent with an AVM. (Focal hyperintensity in the left lateral ventricle is most likely caused by a CSF pulsation artifact, which was also seen on control images.)

B and C, Clotted IVH is markedly hyperintense and easily seen on T1-weighted image (450/20/2) (B). The IVH is markedly hypointense on T2-weighted image (2000/120/2) (C). The T1- and T2-weighted imaging appearances are consistent with the predominantly intracellular methemoglobin content of the IVH.

D, Noncontrast CT scan shows calcified AVM and clotted IVH, each hyperdense.



was seen as layered fluid-fluid levels, which could be distinguished from CSF pulsation artifacts.

For the 40 control subjects, the lateral ventricles in 98%, the third ventricle in 80%, and the fourth ventricle in 72% did not show any significant CSF pulsation artifacts. That is, the ventricular cavity was uniformly hypointense. Furthermore, in none of the control subjects was definite IVH falsely diagnosed. Equivocal hyperintensity (grade 1) was seen in the lateral ventricle in 2% ($n = 1$), in the third ventricle in 20% ($n = 8$), and in the fourth ventricle in 28% ($n = 11$) of the control subjects. This meant that CSF pulsation artifacts were present to some degree, preventing the unequivocal exclusion of IVH. These artifacts were seen as patchy, round, nonlayered hyperintensities on the images of both the patients (Figs 1 and 2) and the control subjects (not shown). An example of a third ventricular CSF pulsation artifact is shown in Figure 1. However, in the control subjects, all lateral ventricles were rated as normal, except one that was rated as grade 1. An example of a lateral ventricular CSF pulsation artifact is shown in Figure 2. The reason that the raters did not diagnose definite IVH in any of the control subjects was the small size and focality of the abnormal hyperintensity that was typical of artifacts and the lack of abnormal fluid-fluid levels that were seen in association with definite IVH. Although fourth ventricular CSF pul-

sation artifacts were not falsely diagnosed as IVH, no patient with fourth ventricular IVH was identified in this series for comparison with controls. Thus, this study did not ascertain whether a fourth ventricular CSF pulsation artifact would affect the sensitivity of diagnosing fourth ventricular IVH.

Discussion

IVH is usually secondary to associated parenchymal hematoma. In addition, primary (solitary) IVH may occur without associated parenchymal bleeding. In the present study, we have shown that the fast FLAIR technique readily detects acute IVH in both primary and secondary forms, and is at least comparable to CT during the acute stage. The FLAIR technique detects acute and subacute IVH with high efficacy and high reliability, particularly in the lateral ventricles. Previous work indicates that the FLAIR technique reliably detects acute (12, 13), subacute (14), and chronic (14) SAH. Similarly, we found that FLAIR MR imaging clearly showed all acute and subacute SAH in our series (Figs 1 and 3). FLAIR MR imaging was superior to CT (showed the lesion more conspicuously) in all cases of acute IVH and in all cases of acute/subacute SAH (Figs 1 and 3). FLAIR MR imaging showed two cases of IVH that were not detected by CT. Although the FLAIR technique is less ef-

fective in showing subacute IVH, detection improves when FLAIR images are combined with T1- and T2-weighted images (Fig 2). In cases of subacute IVH, although FLAIR MR imaging has a high sensitivity in diagnosing IVH, CT was superior in three cases (Figs 2 and 4) and detected one case of IVH that was missed by FLAIR (Fig 4). FLAIR MR imaging also seems to have high specificity in diagnosing IVH. No FLAIR studies of control subjects falsely depicted IVH. Thus, MR studies that include the FLAIR technique seem to be effective and reliable in the diagnosis of acute/subacute IVH, including cases with coexisting SAH, and, in some instances, are superior to CT studies.

The usefulness of FLAIR in the diagnosis of acute IVH and SAH relates to the hyperintense appearance of these types of hemorrhage against a dark CSF background, allowing blood to be seen in ventricles and in sulci (Figs 3A and 3B). This hyperintense appearance of acute IVH and SAH on FLAIR images may relate to several factors that have been reviewed by Noguchi et al (14), including the effects on both T1 and T2 relaxation. The FLAIR technique produces strong T2-weighted images that are highly sensitive to T2 prolongation in tissue. This T2 prolongation in cases of IVH and SAH probably results from a high protein content in these compartments because of the presence of blood and inflammation in both dilute and dense blood-CSF admixtures (14–16). Oxyhemoglobin, the initial product of blood degradation after vascular rupture, may contribute to T2 prolongation (15). The FLAIR hyperintensity may also relate to T1 effects. For example, T1 shortening of dense bloody CSF is more readily shown on FLAIR images than on conventional T1-weighted images (14). FLAIR MR imaging detects small differences in T1 relaxation time in bloody CSF versus normal CSF, which makes dense blood-CSF collections appear hyperintense relative to gray matter (14). Furthermore, T1 shortening may interfere with the FLAIR suppression of dilute bloody CSF (14). Thus, several hypotheses explain the FLAIR hyperintensity of acute IVH/SAH, and although we believe that high protein content plays a major role, this requires further study.

Although acute (first 48 hours) IVH was always hyperintense on FLAIR images, the subacute IVH appearance was variable. Although most patients had essentially hyperintense IVH ($n = 9$), four (31%) had isointense ($n = 1$) (Fig 4A), mixed ($n = 1$), or hypointense ($n = 2$) (Fig 2A) IVH. These other appearances most likely relate to the continuation of blood hemoglobin degradation that is known to add complexity to the MR signal of ICH (15, 17, 18). The degradation of blood after vascular rupture proceeds in proposed stages (15) based on the oxidative state of hemoglobin. Hemoglobin in the RBC fluctuates between an oxygenated and a deoxygenated state, depending on blood oxygen tension (15, 17, 18). Oxyhemoglobin

is the first blood product that predominates after vascular rupture and is most likely hyperintense on FLAIR images because of T2 prolongation. Subsequent conversion to deoxyhemoglobin and intracellular methemoglobin results in T2 shortening, which may be responsible for the change in FLAIR signal to isointense and hypointense (Fig 2A). Consistent with this hypothesis, FLAIR MR images did not show IVH as isointense and hypointense during the first 48 hours after ictus, when oxyhemoglobin is likely to predominate because of the high oxygen and glucose content of the ventricular cavity (19). After the first 48 hours, isointense or hypointense IVH on FLAIR images was associated with an isointense or hyperintense appearance on T1-weighted images and an isointense or hypointense appearance on T2-weighted images (Figs 2 and 4), suggesting that blood had converted to deoxyhemoglobin or intracellular methemoglobin (15, 20–22). Although in vitro studies indicate that these blood degradation products form in CSF (23), we did not obtain direct evidence of the oxidative hemoglobin state in these cases of IVH. Other hypotheses have been offered for the MR signal changes in hematomas over time, such as changes in RBC hydration and alterations in local hematocrit (17). Because of the paucity of data regarding the MR degradation patterns of IVH, our explanations for the dynamic variance in the FLAIR appearance are speculative. Convincing explanations for the FLAIR signal characteristics of IVH at the various stages may require high-field MR animal or phantom model studies.

Surprisingly, little has been written about the degradation pattern and MR appearance of IVH (24–27). In the present study, IVH tended to occur in a layered form, causing blood-CSF (fluid-fluid) levels in the dependent portions of the lateral ventricles, most commonly the occipital horns. This blood-fluid level has also been called the fluid-precipitate level (27) and is most likely caused by different densities of blood components and CSF. In each patient with layered IVH, blood signal assumed the dependent position. This is consistent with the in vivo phenomenon that RBCs assume a dependent position in a test tube, whereas serum/fluid and plasma assume a nondependent position (22). The high rate of layering instead of frank clot formation in association with IVH most likely relates to the intrinsic antithrombotic capability of the CSF because of a high concentration of fibrinolytic activators (17). Recognition of both primary and secondary forms of IVH has prognostic value (28–32) and may help to select patients for novel interventional IVH therapies (33, 34).

An important pitfall in the use of FLAIR MR imaging in the diagnosis of subarachnoid and intraventricular diseases is the CSF pulsation artifact, especially in the posterior fossa. In the present study, we were careful to assess whether this

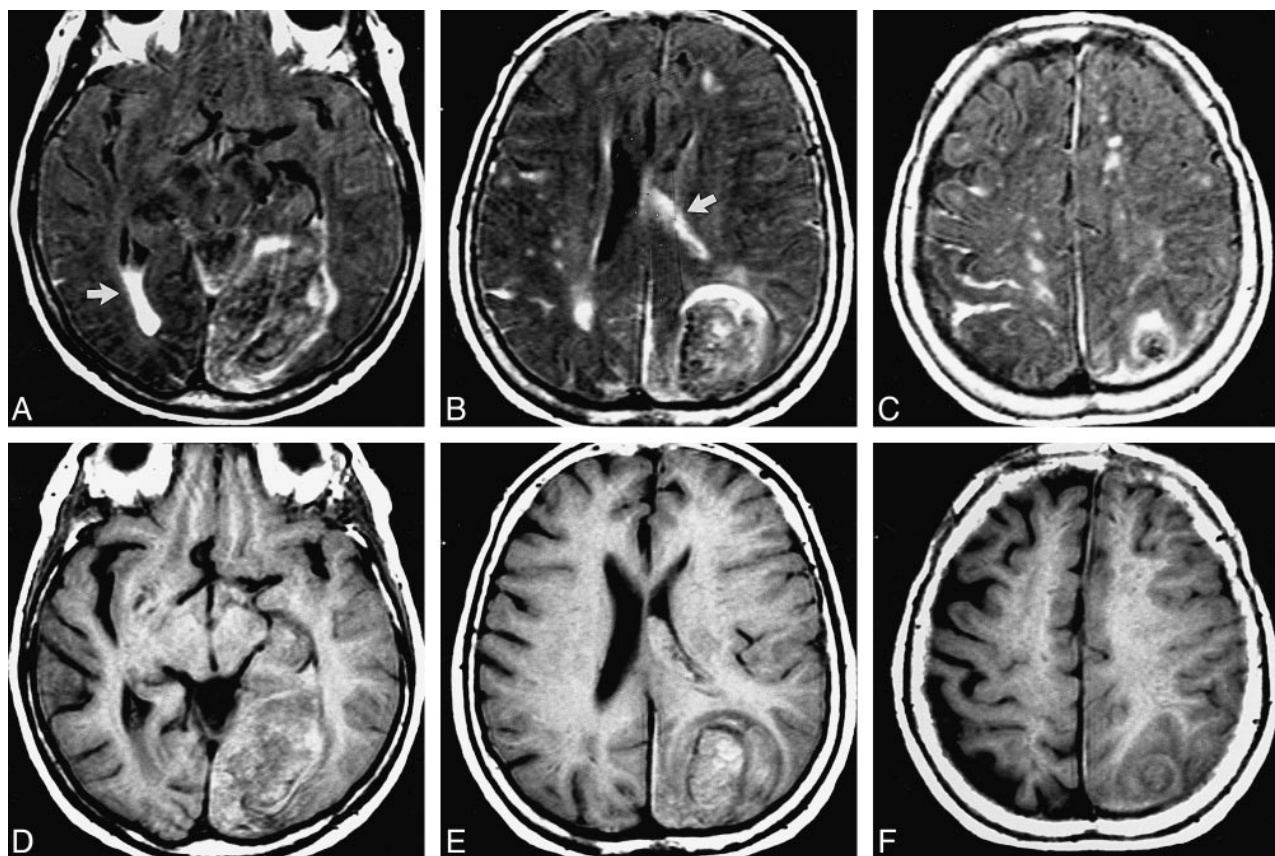


FIG 3. Case 2: 79-year-old woman with acute IVH, intraparenchymal hemorrhage, and SAH who had imaging on the day of ictus. MR and CT studies were obtained 2 hours apart. The FLAIR images show the IVH and SAH better than the T1- and T2-weighted images or the CT scans do.

A–C, FLAIR images (6700/150/2, $T1 = 2200$) show large left parietooccipital intraparenchymal hemorrhage with intraventricular extension and associated SAH. The intraparenchymal hemorrhage is of mixed signal (mostly isointense). However, the IVH is well seen as hyperintense in the right occipital horn (arrow, A) and left body (arrow, B) of the lateral ventricles. SAH is well seen as hyperintensities in the right dorsal frontoparietal sulci (B and C).

D–F, T1-weighted (450/20/2) (D–F) and T2-weighted (2000/120/2) (G–I) images do not show the IVH and SAH as conspicuously as the FLAIR images do.

J–L, Noncontrast CT scans readily show the hyperdense intraparenchymal hemorrhage. However, the IVH and SAH are shown more conspicuously on the FLAIR images.

bright artifact could potentially compromise the usefulness of the FLAIR technique in diagnosing IVH. Most important, IVH was not falsely diagnosed in any of the control subjects. Although CSF pulsation artifacts (Figs 1A and 2A) were common in the third and fourth ventricles and rarely in the lateral ventricle, these findings were not confused with IVH, mainly because of focality and the lack of fluid-fluid levels. However, we studied only two cases of third ventricular IVH and no case of fourth ventricular IVH. Thus, although CSF pulsation artifacts do not seem to compromise the usefulness of FLAIR MR imaging in diagnosing lateral ventricular IVH, we cannot comment on the ability of FLAIR to detect IVH amid prominent CSF pulsation artifacts in the third and fourth ventricles. Additional work is necessary to determine whether a CSF pulsation artifact could reduce the sensitivity of diagnosing third or fourth ventricular IVH. Furthermore, although none of the images had

false-positive findings, it is possible that a CSF flow artifact anywhere in the ventricles might still be confused with IVH in a larger series of patients.

Other limitations of this study are noteworthy. Because this study was retrospective, we did not perform serial MR imaging for every patient, which would have allowed an analysis of intrasubject MR imaging evolution across the major acute and subacute IVH degradation stages. A prospective study of consecutive patients with frequent serial imaging is therefore desirable to understand the temporal evolution of FLAIR appearances. This study does not firmly establish the specificity of FLAIR MR imaging in the diagnosis of IVH. Further studies will be necessary to determine whether the FLAIR appearance will separate IVH from other disease states causing abnormal intraventricular signal, such as neoplasia (35) and ventricular empyema (pyocephalus) (36).

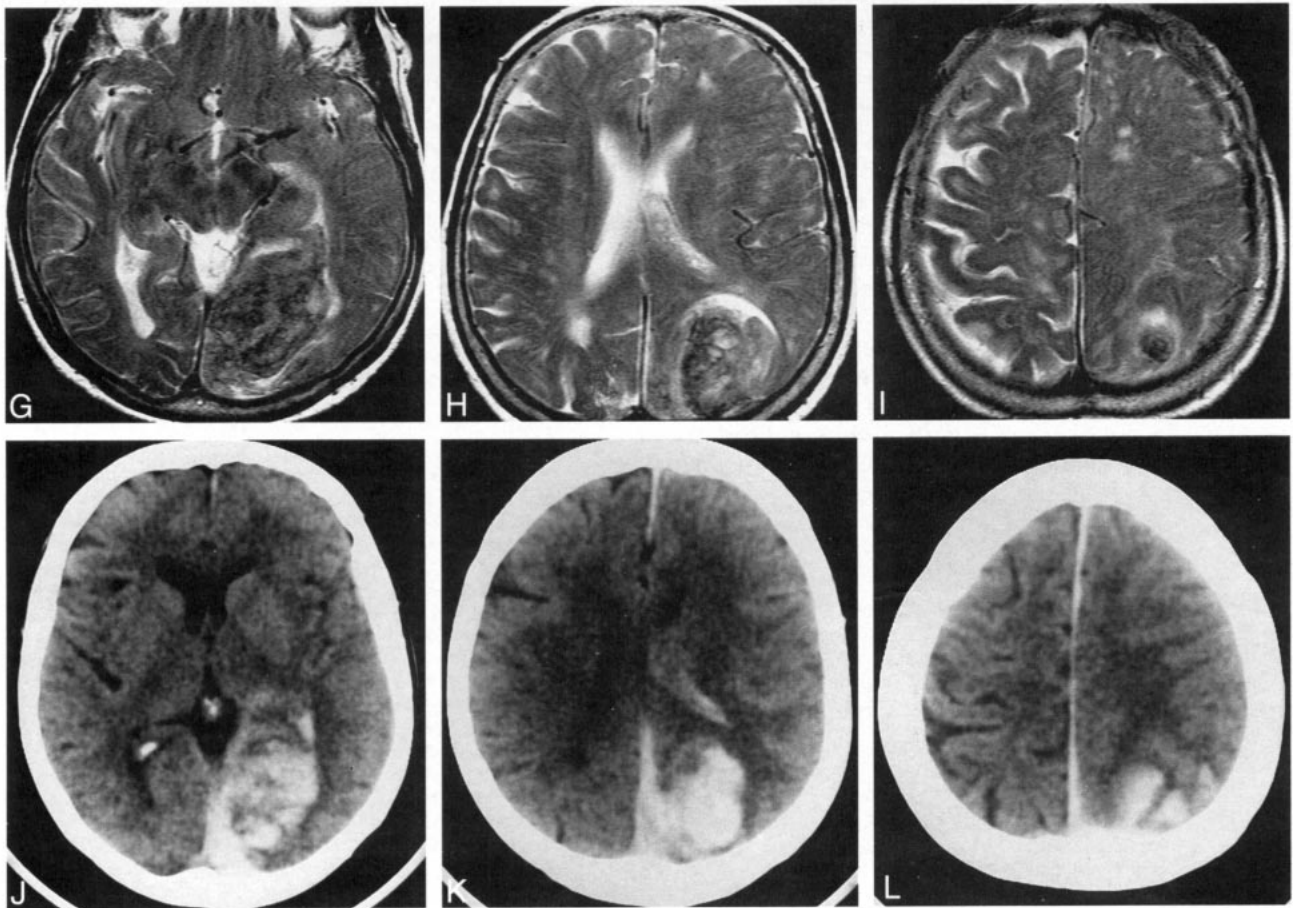


FIG 3. Continued

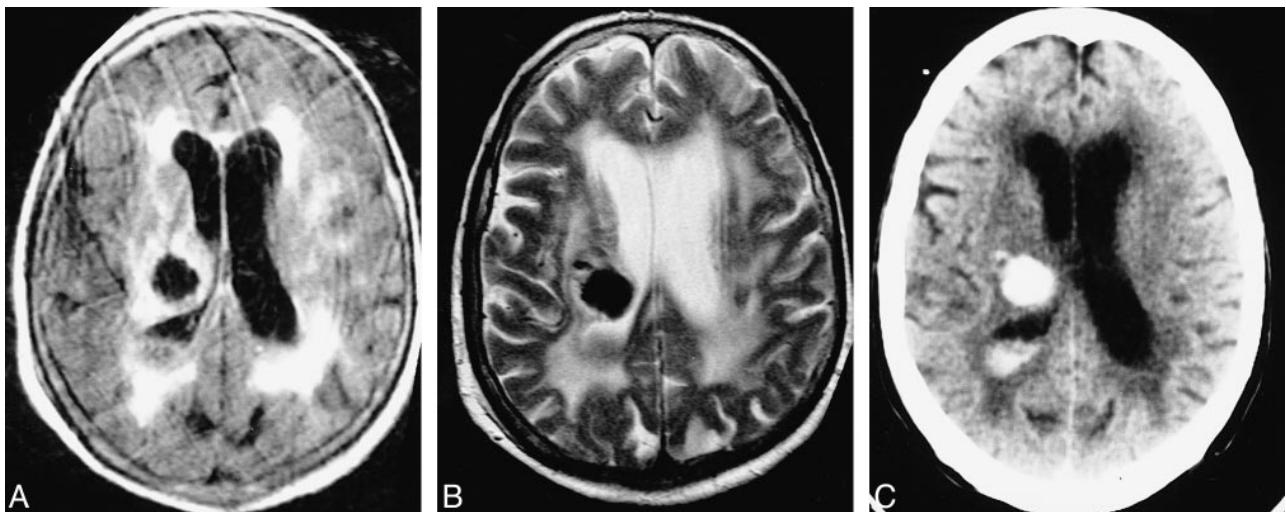


FIG 4. Case 9: 82-year-old woman with subacute IVH and intraparenchymal hemorrhage who had imaging 5 days after ictus. MR images and a CT scan were obtained 2 hours apart. The CT scan shows the IVH better than the MR images do.

A and B, Layered IVH is isointense with gray matter on all three MR sequences and is thus inconspicuous on the FLAIR image (6700/150/2, TI = 2200) (A), the T2-weighted image (2000/120/2) (B), and the T1-weighted image (450/20/2) (not shown).

C, Noncontrast CT scan readily shows the hyperdense intraparenchymal hemorrhage and hyperdense ipsilateral layered IVH. The IVH is more conspicuous on the CT scans than on the MR images.

Conclusion

These findings suggest that MR imaging studies, including fast FLAIR sequences, are highly sensitive and specific in the detection of acute and subacute IVH and coexisting SAH. The fast FLAIR technique is especially useful in identifying acute IVH during the first 48 hours after ictus, in a manner that is at least comparable to CT. FLAIR MR imaging may detect IVH that is missed by CT. For patients presenting with subacute neurologic deterioration, correlating the findings of fast FLAIR with those of T1- and T2-weighted imaging will identify most cases of IVH, although CT may still be necessary to exclude small IVH. CSF pulsation artifacts do not seem to significantly compromise the sensitivity and specificity of FLAIR images in diagnosing IVH in the lateral ventricles.

Acknowledgments

We thank our Millard Fillmore Hospital physician colleagues for referring these patients. We also thank Kim Marie Malicki, Evelyn Calderon, Dolly Sadjak, Janice Tokarczyk, Jennifer Ruske, Joan Schurr, James Pierotti, our MR technologists, and the Kidney Health Sciences Library.

References

1. Atlas SW. **MR imaging is highly sensitive for acute subarachnoid hemorrhage. . . not.** *Radiology* 1993;186:319–322
2. Ogawa T, Inugami A, Shimosegawa E, et al. **Subarachnoid hemorrhage: evaluation with MR imaging.** *Radiology* 1993;186:345–351
3. Post MJD. **Fluid-attenuated inversion-recovery fast spin-echo MR: a clinically useful tool in the evaluation of neurologically symptomatic HIV-positive patients.** *AJNR Am J Neuroradiol* 1997;18:1611–1616
4. Brant-Zawadzki M, Atkinson D, Detrick M, Bradley WG, Scidmore G. **Fluid attenuated inversion recovery (FLAIR) for assessment of cerebral infarction: initial clinical experience in 50 patients.** *Stroke* 1996;27:1187–1191
5. Alexander JA, Sheppard S, Davis PC, Salverda P. **Adult cerebrovascular disease: role of modified rapid fluid-attenuated inversion-recovery sequences.** *AJNR Am J Neuroradiol* 1996;17:1507–1513
6. Filippi M, Yousry T, Baratti C, et al. **Quantitative assessment of MRI lesion load in multiple sclerosis: a comparison of conventional spin-echo with fast fluid-attenuated inversion recovery.** *Brain* 1996;119:1349–1355
7. Filippi M, Horsfield MA, Rovaris M, et al. **Intraobserver and interobserver variability in schemes for estimating volume of brain lesions on MR images in multiple sclerosis.** *AJNR Am J Neuroradiol* 1998;19:239–244
8. Tsuchiya K, Inaoka S, Mizutani Y, Hachiya J. **Fast fluid-attenuated inversion-recovery MR of intracranial infections.** *AJNR Am J Neuroradiol* 1997;18:909–913
9. Thurnher MM, Thurnher SA, Fleischmann D, et al. **Comparison of T2-weighted and fluid-attenuated inversion-recovery fast spin-echo MR sequences in intracerebral AIDS-associated disease.** *AJNR Am J Neuroradiol* 1997;18:1601–1609
10. Bakshi R, Bates VE, Mechtler LL, Kinkel PR, Kinkel WR. **Occipital lobe seizures as the major clinical manifestation of reversible posterior leukoencephalopathy syndrome: magnetic resonance imaging findings.** *Epilepsia* 1998;39:295–299
11. Abe K, Fugimura H, Soga F. **The fluid-attenuated inversion recovery pulse sequence in assessment of central nervous system involvement in myotonic dystrophy.** *Neuroradiology* 1998;40:32–35
12. Noguchi K, Ogawa T, Inugami A, Toyoshima H, Okudera T, Uemura K. **MR of acute subarachnoid hemorrhage: a preliminary report of fluid-attenuated inversion-recovery pulse sequence.** *AJNR Am J Neuroradiol* 1994;15:1940–1943
13. Noguchi K, Ogawa T, Inugami A, et al. **Acute subarachnoid hemorrhage: MR imaging with fluid-attenuated inversion recovery pulse sequences.** *Radiology* 1995;196:773–777
14. Noguchi K, Ogawa T, Seto H, et al. **Subacute and chronic subarachnoid hemorrhage: diagnosis with fluid-attenuated inversion-recovery MR imaging.** *Radiology* 1997;203:257–262
15. Bradley WG. **MR appearance of hemorrhage in the brain.** *Radiology* 1993;189:15–26
16. Melhem ER, Jara H, Eustace S. **Fluid-attenuated inversion recovery MR imaging: identification of protein concentration thresholds for CSF hyperintensity.** *AJR Am J Roentgenol* 1997;169:859–862
17. Hayman LA, Pagani JJ, Kirkpatrick JB, Hinck VC. **Pathophysiology of acute intracerebral and subarachnoid hemorrhage: applications to MR imaging.** *AJNR Am J Neuroradiol* 1989;10:457–461
18. Kirkpatrick JB, Hayman LA. **Pathophysiology of intracranial hemorrhage.** *Neuroimaging Clin North Am* 1992;2:11–23
19. Fishman RA. **Cerebrospinal Fluid in Diseases of the Nervous System.** 2nd ed. Philadelphia: Saunders; 1992:217–234
20. Gomori JM, Grossman RI, Goldberg HI, Zimmerman RA, Bilaniuk LT. **Intracranial hematomas: imaging by high-field MR.** *Radiology* 1985;157:87–93
21. Gomori JM, Grossman RI. **Mechanisms responsible for the MR appearance and evolution of intracranial hemorrhage.** *Radiographics* 1988;8:427–440
22. Cohen MD, McGuire W, Cory DA, Smith JA. **MR appearance of blood and blood products: an in vitro study.** *AJR Am J Roentgenol* 1986;146:1293–1297
23. Bradley WG, Schmidt PG. **Effect of methemoglobin formation on the MR appearance of subarachnoid hemorrhage.** *Radiology* 1985;156:99–103
24. Bakshi R, Kamran S, Kinkel PR, Bates VE, Mechtler LL, Belani S, Kinkel WR. **MRI findings in cerebral intraventricular hemorrhage: analysis of 50 consecutive cases.** *Neuroradiology*. In press
25. Spetzger U, Mull M, Sure U, Gilsbach J. **Subarachnoid and intraventricular hemorrhage caused by hypernephroma metastasis, accompanied by innocent bilateral posterior communicating artery aneurysms.** *Surg Neurol* 1995;44:275–278
26. Bakshi R, Lindsay BD, Kinkel PR. **Brain magnetic resonance imaging in clinical neurology.** In: Joynt RJ, Griggs RC, eds. *Clinical Neurology*. Philadelphia: Lippincott-Raven; 1997:1–203
27. Abrahams JJ, Lidov M, Artiles C. **MR imaging of intracranial fluid levels.** *AJNR Am J Neuroradiol* 1989;10:695–702
28. Tuhim S, Dambrosia J, Price T, et al. **Intracerebral hemorrhage: external validation and extension of a model for prediction of 30-day survival.** *Ann Neurol* 1991;29:658–663
29. Jayakumar PN, Taly AB, Bhavani UR, Arya BYT, Nagaraja D. **Prognosis in solitary intraventricular haemorrhage.** *Acta Neurol Scand* 1989;80:1–5
30. Broderick J, Brott T, Duldner J, Tomsick T, Huster G. **Volume of intracerebral hemorrhage: a powerful and easy-to-use predictor of 30-day mortality.** *Stroke* 1993;24:987–993
31. Shapiro S, Campbell R, Scully T. **Hemorrhagic dilation of the fourth ventricle: an ominous predictor.** *J Neurosurg* 1994;80:805–809
32. Young WB, Lee KP, Pessin MS, Kwan ES, Rand WM, Caplan LR. **Prognostic significance of ventricular blood in supratentorial hemorrhage: a volumetric study.** *Neurology* 1990;40:616–619
33. Rohde V, Schaller C, Hassler W. **Intraventricular recombinant tissue plasminogen activator for lysis of intraventricular haemorrhage.** *J Neurol Neurosurg Psychiatry* 1995;58:447–451
34. Findlay J, Grace M, Weir B. **Treatment of intraventricular hemorrhage with tissue plasminogen activator.** *Neurosurgery* 1993;32:941–947
35. Lang I, Jackson A, Strang FA. **Intraventricular hemorrhage caused by intraventricular meningioma: CT appearance.** *AJNR Am J Neuroradiol* 1995;16:1378–1381
36. Bakshi R, Kinkel PR, Mechtler LL, Bates VE. **Cerebral ventricular empyema associated with severe adult pyogenic meningitis: computed tomography findings.** *Clin Neurol Neurosurg* 1997;99:252–255